# Effects of Ion Implantation on Microstructure, Endurance and Wear Behavior of IBAD $MoS_2$

K.J. Wahl, D.N. Dunn*, and I.L. Singer

*Code 6176, Naval Research Laboratory, Washington DC 20375-5342*

**Dept. of Materials Science and Engineering, University of Virginia, Charlottesville, VA 22903*

## ABSTRACT

Thin $MoS_2$ coatings were prepared on steel and Si substrates via ion-beam assisted deposition using conditions known to produce dense, basal oriented microstructures. After deposition, the coated substrates were irradiated with 180 keV $Ar^{++}$ ions at doses of $1x10^{15}$, $1x10^{16}$, and $5x10^{16}$ ions/cm$^2$. Microstructures of as-deposited and ion irradiated $MoS_2$ coatings were examined using x-ray diffraction, high resolution transmission electron microscopy, and micro-Raman spectroscopy. Friction, wear and endurance were examined under both unidirectional and reciprocating sliding conditions in dry air. The lowest ion irradiation dose altered the initial microstructure, producing basal oriented, nearly defect-free crystalline domains of $MoS_2$ in an amorphous matrix; at the highest dose the coatings were nearly amorphous, but the remaining $MoS_2$ showed mixed orientation. Ion irradiation of the $MoS_2$ coatings did not significantly modify the friction behavior, and only at the highest dose was the endurance altered, decreasing by more than 75%. Two changes in wear behavior were observed in the highest dosed coatings: 1) accelerated wear of the coating and 2) elimination of solid lubricant reservoirs. Destruction of the solid lubricant replenishment process resulted in premature failure of the highest dosed coating.

**Keywords:** wear, molybdenum disulphide, $MoS_2$, solid lubrication, ion irradiation

*Submitted to Wear, June 1999; Accepted October 1999*

## INTRODUCTION

Microstructure is reported to be a controlling factor in the friction and endurance of $MoS_2$ coatings. [1-6]. So, it is not surprising that ion irradiation, which can dramatically alter the microstructure of $MoS_2$, can also affect its tribological properties. Irradiation of sputter deposited coatings having porous, low density, edge oriented columnar plate morphology and low film-substrate adhesion invariably results in improved coating endurance [7-18]; similar experiments have been described for $WS_2$ [19]. However, careful studies by Mikkelsen and Sørensen [20] have demonstrated that while ion irradiation both densified and increased the endurance of poor (porous, edge-oriented) $MoS_2$ coatings, the same treatment applied to better performing sputtered coatings (with dense, nearly amorphous microstructures) resulted in decreased endurance at high dosages. Furthermore, they showed that ion irradiation brought all coatings, both high and low quality, to nearly the same density and endurance.

Fully dense $MoS_2$ coatings can also be produced by using energetic beams during sputter deposition. Singer and co-workers used 1 keV $Ar^+$ ion-beam assisted deposition (IBAD) to produce dense $MoS_2$ coatings that also have basal textured microstructures [21-23]. These coatings show better endurance than many sputtered coatings [24]. Wear studies have shown that the IBAD $MoS_2$ coatings wear in three stages [25, 26]. In Stage I the coatings initially resist wear. Rapid wear takes place in Stage II, often within the first 10% of sliding life and results in loss of 50% or more of the initial coating thickness. Such early wear is similar to that of other $MoS_2$ coatings in both sliding [4, 5, 27-29] and rolling contact [30]. In Stage III, the net wear of the coating is low, due to resupply of $MoS_2$ to the contact via lubricant reservoir dynamics.

The purpose of this study is to examine the effects of ion irradiation on the microstructure and tribological behavior of dense, adherent, basal oriented IBAD $MoS_2$ coatings. Can these coatings be improved by ion irradiation, or will their performance be degraded as were the better performing sputtered coatings of Mikkelsen and Sørensen [20]? An IBAD $MoS_2$ coating was-deposited on several substrates simultaneously and modified by ion irradiation using the same conditions Mikkelsen and Sørensen [20] found to alter coating microstructure from crystalline to amorphous. The resulting microstructural and tribological changes were examined via optical

microscopy, Raman spectroscopy, high resolution transmission electron microscopy (HRTEM) and x-ray diffraction (XRD). Both unidirectional and reciprocating sliding tests were performed to evaluate friction and wear behavior. The effects of irradiation on microstructure and tribological performance are correlated and discussed in terms of wear resistance and lubricant reservoir dynamics.

## EXPERIMENTAL

IBAD $MoS_2$ coatings were simultaneously deposited over a TiN interlayer onto 9 polished substrates: three 52100 steel, three M50 steel and three Si. Deposition conditions were chosen to produce dense, basally oriented coatings (substrate temperature 200°C, ion-to-atom ratio 0.046) [22] while the TiN layer served as a diffusion barrier during elevated temperature deposition [31]. After deposition, coated steel and Si substrates were irradiated at room temperature with 180 keV $Ar^{++}$ ions (equivalent to 360 keV $Ar^{+}$ ions) at doses of 1 x $10^{15}$ and 1 x $10^{16}$ ions/$cm^2$; coated samples from each of the different substrates were kept in the as-deposited condition to serve as references. Later, the samples irradiated to 1 x $10^{15}$ ions/$cm^2$ were implanted a second time to achieve a final dose of 5 x $10^{16}$ ions/$cm^2$. The irradiated coatings will be referred to as low dose (LD), high dose (HD) and ultra-high dose (UHD), respectively.

Ar ion implantation profiles were computed using Profile Code (Implant Sciences, Ver. 3.2) [32]. Implant concentration and range distributions for four doses of 360 keV $Ar^{+}$ into a 185 nm $MoS_2$ layer on Si are shown in Fig. 1. The majority of Ar ions passed through the $MoS_2$ layer, with the peak concentration found in the Si at a range of about 300 nm. In $MoS_2$, the maximum concentration of Ar was found at the $MoS_2$/Si interface. At the highest dose used in the present experiment, 5 x $10^{16}$ ions/$cm^2$, the Ar concentration at the interface was about 7 x $10^{20}$ atoms/$cm^3$, or 2 at. %. In addition, calculations predicted a sputtering rate of 0.59 nm per 1 x $10^{15}$ Ar ions, which would result in about 30 nm of $MoS_2$ removed at the highest dose. Damage profiles for this implantation treatment were computed with TRIM (Version 96.5) [33]. The maximum damage density occurred at the $MoS_2$/Si interface, where about 0.14 atomic displacements/ion/nm took place. $MoS_2$ received a higher damage density than Si only because it has a greater atomic density than Si.

As-deposited and ion irradiated coatings were examined using XRD, Raman spectroscopy and HRTEM techniques. XRD was performed in standard $\theta/2\theta$ configuration with Cu $K_\alpha$ radiation. Raman spectra were obtained on a Renishaw imaging microscope at low power (less than 25 mW) with an $Ar^+$ ion laser with a wavelength of 514 nm and 1 $cm^{-1}$ spectrometer resolution. Cross-section TEM samples were made from the Si coated substrates via standard techniques [34] and examined using a Hitachi H-9000 at 300 keV operated in imaging and selected area electron diffraction (SAED) modes; images were taken with the aperture encompassing the transmitted beam and (002) reflections.

Friction and wear behavior was evaluated in both unidirectional and reciprocating sliding tests. Sliding endurance and friction behavior for the coatings deposited on steel substrates were measured under unidirectional sliding conditions with a pin-on-disk (POD) tribometer. 52100 steel balls (3.18 mm diameter) were solvent cleaned and loaded against the specimens to 9.8 N, resulting in a mean Hertzian stress of $P_H$ = 1.4 GPa (maximum $P_H$ = 2.1 GPa). Tests were performed in dry air at sliding speeds of 0.2 to 0.6 m/s. Coating endurance was defined as the number of revolutions before the friction coefficient reached 0.2. At least 3 endurance tests were performed for each coating. Additional sliding experiments were performed using a reciprocating ball-on-flat tribometer with 6.35 mm diameter 52100 steel balls and initial load of 9.8 N (mean $P_H$ = 0.92 GPa, max $P_H$ = 1.4 GPa). Sliding speed was 4 mm/s and track lengths 3-5 mm; endurance was defined as the number of reciprocating cycles before an average friction coefficient of 0.2 was reached, as in the POD tests. Between 1 and 3 reciprocating endurance tests were run for the as deposited, HD and UHD coatings. Reciprocating sliding tests up to 30000 cycles were performed using what we call the “stripe” testing methodology, described previously [25] and shown schematically in Fig. 2. Briefly, each track was run a length of 5 mm for the first $n$ = {1,3,10,30,100,…} cycles, and then the stroke length was shortened to 3 mm for an additional 2$n$ cycles; a new ball was used for each track. The result of using this test configuration is that 1) each track contains three turnaround points (instead of the normal two in a reciprocating track, with the extra turnaround point in the middle), and 2) multiple wear tracks run to the same number of sliding cycles are obtained with minimal number of tests and coating area needed.

Coating wear tracks and transfer films on balls were examined optically with a Nomarski microscope. Coating thickness and wear track depths were measured to within 10 nm using Michelson interferometry (MI).

## RESULTS

### Structural Analyses of Coatings

The as-deposited, LD and HD coating thicknesses, measured by MI, were all roughly 200 nm, while the UHD coating was 180 nm thick. We attribute the 20 nm reduction in thickness to sputtering losses (roughly that predicted by Profile Code calculations) rather than coating compaction, because the as-deposited IBAD $MoS_2$ coatings are fully dense [35].

Raman spectra of three coatings (as-deposited, LD and UHD) are shown in Fig. 3a. All spectra exhibited Raman bands similar to those for molybdenite [36], but intensity of the bands decreased in the ion irradiated coatings.

Figure 3b shows XRD spectra of as-deposited and ion irradiated coatings. The as-deposited coating had two peaks: a broad peak at 13.52° and a low 2θ peak at 11.02°. Both peaks have been observed previously in IBAD $MoS_2$ [22]. The LD and HD ion irradiated coatings exhibited only a narrower (002) peak at 14.25°, with reduced intensity as dosage was increased. The UHD coating spectra showed no crystalline $MoS_2$ peaks at all. The peak at 13.52° in the as-deposited coating is identified as the (002) peak of $MoS_2$, and yields d-spacings similar to those reported for other sputtered $MoS_2$ films. Recently, Dunn et al. [34] have attributed the low 2θ peak in the as-deposited coating to widely spaced $MoS_2$ basal planes resulting from defects in the coating crystal structure. These defects were removed in the ion irradiated coatings, sharpening and shifting the (002) peak towards that of crystalline $MoS_2$.

Figure 4 is a montage of multi-beam images from cross-sectional TEM of as-deposited, LD, and UHD coatings. Figures 4a and 4b are taken with the objective aperture encompassing the transmitted beam and (002) reflections, while Fig. 4c is taken without an objective aperture. SAED patterns inset in each image were taken from the same area as each image.

The as-deposited coating (Fig. 4a) shows basal-oriented, nanocrystalline domains of $MoS_2$, with numerous forked and terminated plane defects [23, 34]. The horizontal fringes

observed in the images correspond to individual S-Mo-S layers and are due to interference between (002) reflections. The SAED pattern inset in Fig. 4a consists of two sets of arcs. The larger, diffuse arcs correspond to (002) reflections, and the smaller, inner arcs are due to expanded basal plane spacing arising from fork and termination defects [34].

The TEM image of the LD coating (Fig. 4b) shows small domains of basal oriented crystallites embedded in an amorphous matrix. Remaining crystalline regions show fewer fork and termination defects. SAED of the LD film shows only well defined (002) reflections. In comparison with (002) reflections in Fig. 4a, these reflections are sharper and shifted outward in reciprocal space. This implies that the (002) spacing of the crystalline regions has contracted and that these regions have far fewer defects than in the as-deposited coating. In addition, the inner reflection seen in the SAED pattern in Fig. 4a has vanished, consistent with XRD spectra in Fig. 3 and previous results [34].

At the highest implantation dose (UHD, Fig. 4c), the coating still contained crystalline regions. Basal planes were oriented in many directions, and (100) fringes were also observed at several orientations. Circular areas of amorphous material can also be seen by their light contrast. Moreover, basal planes appeared at the circumference of several of the circles. The SAED pattern shows a strong, diffuse background with weak, diffuse spots near the transmitted beam. These spots are due to remaining crystalline regions and can be indexed as (002) reflections. The combination of a strong diffuse background and weak, low intensity (002) reflections implies that the UHD coating is mostly amorphous with a few small remnant crystalline regions. Additionally, the positions of the (002) reflections indicate that many of the basal planes are no longer oriented parallel to the substrate.

**Friction, wear, and endurance**

Results of unidirectional (POD) and reciprocating sliding experiments are shown in Fig. 5; error bars are standard deviations calculated from at least 3 POD tests and 2 reciprocating tests (only one reciprocating endurance test was performed for the UHD coating). For both types of tests, only the UHD coating showed a large drop (by more than 75%) in endurance. POD

endurance of the HD coating was slightly higher than both the as-deposited and LD coatings. However, this trend was not reproduced in reciprocating tests.

Unlike sliding endurance, steady state friction coefficients of the various coatings were not affected by ion irradiation. Steady state friction coefficients for POD tests were about 0.02. Friction coefficients for reciprocating tests fell to between 0.02 and 0.04 for all coatings tested by 100 cycles; however, subtle differences in run-in behavior were observed. Friction coefficients from reciprocating sliding are plotted in Fig. 6. After irradiation, the first cycle friction was higher for both the HD and UHD coatings. Also, there was more variability during the first 10 cycles for the HD coating. However, the friction evolution for each of the implantation treatments was similar, indicating good reproducibility of the stripe test method.

Wear depths of tracks from reciprocating sliding tests of the as-deposited (■), HD (▲), and UHD (●) coatings are shown in Fig. 7. Data points represent maximum wear track depth, but do not include depths of narrow (~5 μm or less) scratches. The as-deposited coating showed no measurable wear up to 100 cycles (what we have previously identified as Stage I [25]). By 1000 cycles (Stage II wear) ~100 nm of coating had been worn away, and by 20000 cycles wear track depths were the full thickness of the coating. The HD coating had similar wear behavior to the as-deposited coating, although the onset of measurable wear was not observed until 300 cycles and the wear depths thereafter were generally lower (~60nm). In contrast, the UHD coating wore much more rapidly: measurable wear occurred by 10 cycles, up to 100 nm of wear by 30 cycles, and failure by ~3700 cycles. Failure of the UHD coating resulted from a deep, narrow scratch through the coating to the steel substrate; only 130 nm of wear had occurred over the bulk of the wear track width.

Representative optical micrographs of ball transfer films after 90 cycles of reciprocating sliding are shown in Fig. 8. Much more coating material had been transferred to the ball after sliding against the UHD coating than either the as-deposited or HD coatings. Figure 9 shows a portion of the central regions of the corresponding wear tracks at 90 cycles and also at 900 cycles. The as-deposited and HD coatings showed similar morphologies: at 90 cycles, only a few scratches and light burnishing were observed, and by 900 cycles both showed scratches and debris lumps. Morphological changes for the as-deposited and HD wear tracks and transfer films were

comparable at all sliding cycles examined between 30 and 9000 cycles. In contrast, the UHD track showed many scratches after as few as 10 cycles (not shown), and was heavily scratched by 90 cycles (Fig. 9).

Figure 10 shows end portions of the reciprocating wear tracks for the three coatings after 30, 300 and 3000 cycles. Wear scars and debris buildup for the as-deposited and HD coatings (10a and b) were consistent with previous experiments under identical sliding conditions [25]; debris accumulated as patches and at track ends under the turnaround points (see regions labeled in Fig. 2), as well as on the track during the period of high wear between ~100-300 and ~1000-3000 cycles. The only noticeable difference between the as-deposited and HD wear track morphology was a slightly "smoother" appearance of the HD track surfaces. The UHD tracks, unlike those of the as-deposited and HD coatings, showed no accumulation of retransferred wear debris on the track surface or under the turnaround points at track ends (Fig. 10c). Fine, loose debris was observed beyond the ends of the UHD tracks; no similar debris was observed for the as-deposited or HD coatings.

In summary, the data indicate a large decrease in endurance and a reduction in wear resistance for UHD coatings, with a slight increase in endurance and wear resistance for HD coatings.

## DISCUSSION

Ion irradiation changed the microstructure of IBAD $MoS_2$ in ways both expected and unexpected. Since the IBAD coatings were fully compact in the as-deposited condition, it was not surprising that ion irradiation did not substantially decrease the thickness of the coatings. Only the UHD coating showed a decrease in thickness, from 200 to 180 nm; this decrease can be fully accounted for by sputtering. TEM showed that irradiation at the lowest doses amorphized regions of the coating but also produced domains of basal oriented $MoS_2$ with fewer defects than the as-deposited coating. While we are not certain of the explanation for this particular transformation, we speculate that the areas with high defect concentrations were amorphized first as they are more stressed than defect free areas, where atoms are in low energy (equilibrium) sites. XRD suggested that higher doses reduced the coating to an amorphous matrix. However, TEM showed

that at the highest dose, the coating contained not only amorphous material, but also mixed-oriented $MoS_2$ crystallites (with very short-range order). The circles of amorphous material and the reorientation of crystallites can be attributed to the high stress levels imparted by the high dose irradiation [37]. Mikkelsen and Sørensen found that doses equivalent to the HD used in this study fully amorphized their $MoS_2$ coatings [20]. Those coatings, however, produced by rf-sputtering in a conventional moderate vacuum system, had from 6-25 at.% O contamination. The higher stability of the IBAD $MoS_2$ to irradiation could be due to their lower contamination levels (typically 1-3 at.%) [35].

Despite the reduction of crystallinity in the coatings, friction coefficients of irradiated coatings achieved the same ultralow value (0.02) as as-deposited coatings. This is consistent with previous studies showing that even fully amorphized $MoS_x$ coatings retained their low friction properties [10, 12]. This is not surprising, as amorphous $MoS_x$ [3, 38] as well as amorphous $MoS_x$ containing PbO [39] or Pb [40-42] have been shown to recrystallize to form $MoS_2$ under sliding stresses. While it had been reported earlier that amorphization of $MoS_2$ increased friction [2, 28], those results have been explained by contamination effects [2, 11].

Although ion irradiation did not significantly alter friction coefficients of IBAD $MoS_2$ coatings, endurance was reduced by 75% or more, but only at the highest dosage. While endurance of poor quality coatings (e.g. porous, non-adherent, or edge-oriented) may be improved through structural changes induced by ion irradiation (densification and/or microstructural transformation), better coatings may not. Experiments by Mikkelsen and Sørensen [11] imply that the benefits of high ion irradiation doses are only realized for the poorest quality films. In their study, as irradiation doses were increased beyond a crystalline-to-amorphous transition region, *sliding endurance for all films approached the same limit*: endurance of better performing coatings decreased while endurance of the poorest coating increased. Our results are consistent with their observations; specifically, dense, adherent IBAD $MoS_2$ coatings remain dense and adherent after irradiation.

What was responsible for the decreased endurance of the UHD coating? Reciprocating sliding tests revealed that decreased endurance was accompanied by both decreased wear resistance and elimination of transfer buildup (including end patches) on tracks. We do not

attribute the reduced endurance to earlier wear of the coating, nor to the slight decrease in available lubricant, i.e. the 10% decrease in coating thickness. All the $MoS_2$ coatings (as-deposited and irradiated) wore rapidly early in sliding life (most wear occurred between 30 to 1000 cycles); however, only the UHD coating did not sustain low friction sliding far beyond the high wear stage. Amorphization of the UHD coating cannot fully account for this reduction in endurance, either. Much of the amorphization took place at relatively low irradiation doses (LD and HD), where no decrease in endurance was observed. In addition, previous studies on IBAD $MoS_2$ coatings, produced under various deposition conditions, have shown that endurance of amorphous or nearly amorphous coatings could be nearly as good as basal oriented coatings [6].

The reduced endurance of the UHD coating can be accounted for by a change in the lubricant replenishment process as evidenced by the elimination of transfer buildup on tracks. On the tracks at the turnaround regions, end patches were seen on the as-deposited and LD tracks; the end patches are formed when debris is lost from the ball transfer film when the sliding direction is reversed. Previously, we identified debris patches at track turnaround points and transfer films on balls as lubricant reservoirs [25]. Specifically, we found that through these lubricant reservoirs, low friction sliding was sustained despite rapid, early wear of $MoS_2$ (>50% of the coating worn through in the first 5-10% of sliding life). These lubricant reservoir end patches are absent in the UHD tracks, despite copious amounts of $MoS_2$ debris transferred to the ball. Without the reservoirs and replenishment process, the limited amount of lubricant available to resupply the contact was not sufficient to sustain low friction sliding for long once the coating had worn. Debris patch reservoirs (and not transfer films on the ball) are necessary for the replenishment process to enhance the endurance of $MoS_2$ coatings.

It is likely that the microstructure of the UHD coating was responsible for the absence of end patches retransferred to the track and loss of the replenishment process. Perhaps the ball transfer film formed from the UHD coating adhered to the ball more firmly than transfer films formed from the as-deposited and HD coatings, making it less likely that the ball transfer debris would fall off at the ends of the track when sliding is reversed. While debris extruded beyond the contact zone could fall off the ball, these particles would be ejected beyond the track and could not be reused to relubricate the track. The enhanced adherence of UHD coating material could be

due to the presence of edge-oriented crystallites in the coating. Edge sites of $MoS_2$ are known to be more reactive than basal planes [43] and would bond (and transfer) to the steel ball more readily than basal-oriented crystallites. At the present time, we have not identified the chemistry associated with this hypothesized enhanced adhesion to the ball, although oxidation of these exposed edge sites may increase adhesion of coating material to the sliding counterface [44].

The presence of edge-oriented $MoS_2$ crystallites in the UHD coating not only appears to eliminate the replenishment process and degrade the endurance, but may also contribute to the reduction in wear resistance we observed. Coatings whose worn surfaces expose reactive edge sites may be removed more readily (again, due to adhesion to the counterface) than those exposing only relatively inert basal planes. In our study, accelerated wear and copious debris on the ball counterfaces of the UHD coating are consistent with this model. Alternatively, it is also possible that the mechanical properties of the $MoS_2$ coating have been altered substantially at the highest irradiation dose. For example, ion irradiation is known to reduce hardness and modulus of ceramics as they are amorphized [45-47]. However, we don't believe that simply amorphization of the $MoS_2$ coatings is likely to reduce their wear resistance. Our amorphous, Pb-doped Mo-S coatings [40-42] showed remarkable wear resistance (as little as 40 nm wear in 30000 reciprocating sliding cycles); suggesting that amorphization alone does not control wear of these coatings.

Finally, the slight increase in endurance (POD only) and wear resistance of the HD coatings was intriguing. Small (1.3x to 1.9x) increases in endurance [20] and resistance to wear initiation [12] were observed in the experiments by Mikkelsen and Sørensen. They speculated that the endurance increases were due to enhanced film-substrate adhesion as microstructural changes were minimal. The 1.5x improvement we observed falls within their experimentally observed range of "1.3-1.9" and is possibly significant; however, this same increase was not observed for our reciprocating sliding tests. In our study, it is interesting to consider the possible correlation between slightly increased wear resistance and reduction of defects in the $MoS_2$ crystallites. The microstructural changes might increase hardness at intermediate dosages, as in ceramics [48], and influence deformation of the coatings. Perhaps, as has been suggested previously [5], there is an "optimum" crystallite microstructure or size controlling the wear and endurance of these coatings.

However, in the case of irradiated IBAD $MoS_2$, nanometer scale, rather than micrometer scale, structures may control optimum performance. Further experiments are planned to elucidate mechanical and/or chemical changes (to coatings, worn surfaces, and debris) that are responsible for the altered wear resistance and replenishment processes.

## CONCLUSIONS

Ion irradiation of dense, oriented IBAD $MoS_2$ coatings produced a microstructure with basal oriented crystalline domains of $MoS_2$ in an amorphous matrix. At the highest dose the coatings were nearly amorphous and contained $MoS_2$ crystallites without preferential basal orientation. Ion irradiation of the IBAD $MoS_2$ coatings did not significantly alter the friction coefficient and endurance for better or worse, except at the highest dose, where endurance decreased markedly. The decrease in endurance was associated with two significant changes in tribological behavior: 1) accelerated wear of the coating and 2) elimination of solid lubricant reservoirs. A possible explanation for these behaviors is that the reoriented (non-basal) $MoS_2$ crystallites generated at the highest dose were more readily transferred from the coating and more adherent to ball surfaces. Destruction of the solid lubricant replenishment process resulted in premature failure of the coating irradiated at the highest dosage.

## ACKNOWLEDGMENTS

The authors wish to acknowledge the support of ONR/NRL for funding. The authors also grateful for the experimental contributions of R.N. Bolster, L.E. Seitzman, A. Kyriakopoulos, and Randy Walker. We thank J.F. Ziegler for providing the TRIM code. D.N.D. was supported through the American Society of Engineering Education by an ASEE post-doctoral fellowship.

## REFERENCES

[1] T. Spalvins, Morphological and frictional behavior of sputtered $MoS_2$ films, *Thin Solid Films, 96* (1982) 17-24.

[2] V. Buck, Preparation and properties of different types of sputtered $MoS_2$ films, *Wear, 114* (1987) 263-274.

[3] M.R. Hilton and P.D. Fleischauer, Structural Studies of Sputter-Deposited $MoS_2$ Solid Lubricant Films, in L. Pope, L. Fehrenbacher, and W. Winer, (eds.), *New Materials*

*Approaches to Tribology: Theory and Applications*.: Mater. Res. Soc. Proc., Vol. 140, Materials Research Society, 1989, pp. 227-238.

[4] M.R. Hilton, R. Bauer, and P.D. Fleischauer, Tribological Performance and Deformation of Sputter-Deposited $MoS_2$ Solid Lubricant Films during Sliding Wear and Indentation Contact, *Thin Solid Films, 188* (1990) 219-236.

[5] P.D. Fleischauer and R. Bauer, Chemical and Structural Effects on the Lubrication Properties of Sputtered $MoS_2$ Films, *Tribol. Trans., 31* (1988) 239-250.

[6] L.E. Seitzman, R.N. Bolster, I.L. Singer, and J.C. Wegand, Relationship of Endurance to Microstructure of IBAD $MoS_2$ Coatings on Steel, *Tribol. Trans., 38* (1995) 445-451.

[7] J. Chevallier, S. Olesen, and G. Sørensen, Enhancement of sliding life of $MoS_2$ films deposited by combining sputtering and high-energy ion implantation, *Appl. Phys. Lett., 48* (1986) 876-877.

[8] K. Kobs, H. Dimigen, H. Hübsch, H.J. Tolle, R. Leutenecker, and H. Ryssel, Enhanced Endurance Life of Sputtered $MoS_x$ Films on Steel by Ion Beam Mixing, *Mat. Sci. Eng., 90* (1987) 281-286.

[9] K. Kobs, H. Dimigen, H. Hübsch, and H.J. Tolle, Improved tribological properties of sputtered $MoS_x$ films by ion beam mixing, *Appl. Phys. Lett., 49* (1986) 496-498.

[10] N.J. Mikkelsen, J. Chevallier, and G. Sørensen, Friction and Wear Measurements of Sputtered $MoS_x$ Films Amorphized by Ion Bombardment, *Appl. Phys. Lett., 52* (1988) 1130-1132.

[11] N.J. Mikkelsen and G. Sørensen, Ion Beam Modification of $MoS_x$ Films on Metals, *Mat. Sci. Eng., A115* (1989) 343-347.

[12] N.J. Mikkelsen and G. Sørensen, Modification of molybdenum-disulphide films by ion-bombardment techniques, in L. Pope, L. Fehrenbacher, and W. Winer, (eds.), *New Materials Approaches to Tribology: Theory and Applications*.: Mater. Res. Soc. Proc., Vol. 140, Materials Research Society, 1989, pp. 265-270.

[13] A. Matsui and Y. Kagimoto, Improvement of Tribological Properties of $MoS_2$ Films by Forming Interlayers and/or Bombarding with Ions, in W.D. Nix, *et al.*, (eds.), *Thin Films: Stresses and Mechanical Properties III*, Vol. 239, Materials Research Society, 1992, pp. 605-610.

[14] H.W. Liu and X.S. Zhang, Improved Tribological Properties of Sputtered $MoS_2$ Films Through $N^+$ Implantation, *Thin Solid Films, 240* (1994) 97-100.

[15] H.W. Liu, X.S. Zhang, D.Y. Yu, and X.P. Wang, The Enhancement of Wear Life and Moisture Resistance of Sputtered $MoS_2$ Films by Metal-Ion Implantation, *Wear, 173* (1994) 145-149.

[16] A. Jain and S. Srivastav, Treatment of $MoS_2$ films by high-energy heavy ion beams, *Thin Solid Films, 277* (1996) 128-131.

[17] R.S. Bhattacharya, A.K. Rai, and A. Erdemir, High Energy (MeV) Ion Beam Modifications of Sputtered $MoS_2$ Coatings on Sapphire, *Nuclear Instruments and Methods in Physics Research, B59/60* (1991) 788-792.

[18] R.S. Bhattacharya, A.K. Rai, A.W. McCormick, and A. Erdemir, High Energy (MeV) Ion Beam Modifications of Sputtered $MoS_2$ Coatings on Ceramics, *Tribol. Trans., 36* (1993) 621-626.

[19] A.K. Rai, R.S. Bhattacharya, J.S. Zabinski, and K. Myoshi, A comparison of the wear life of as-deposited and ion-irradiated $WS_2$ coatings, *Surf. Coat. Technol., 92* (1997) 120-128.
[20] N.J. Mikkelsen and G. Sørensen, Solid lubricating films produced by ion bombardment of sputter deposited $MoS_x$ films, *Surf. Coat. Technol., 51* (1992) 118-123.
[21] L.E. Seitzman, R.N. Bolster, and I.L. Singer, X-ray diffraction of $MoS_2$ coatings prepared by ion-beam-assisted deposition, *Surf. Coat. Technol., 52* (1992) 93-98.
[22] L.E. Seitzman, I.L. Singer, and R.N. Bolster, Effects of Temperature and Ion-to-Atom Ratio on the Orientation of IBAD $MoS_2$ Coatings, *Thin Solid Films, 260* (1995) 143-147.
[23] D.N. Dunn, L.E. Seitzman, and I.L. Singer, $MoS_2$ Deposited by Ion Beam Assisted Deposition: 2H or Random Layer Structure?, *J. Mater. Res., 13* (1998) 3001-3007.
[24] S.V. Didziulis, M.R. Hilton, R. Bauer, and P.D. Fleischauer, Thrust Bearing Wear Life and Torque Tests of Sputter-Deposited $MoS_2$ Films, The Aerospace Corporation, Los Angeles, CA, 1992, TOR-92(2064)-1.
[25] K.J. Wahl and I.L. Singer, Quantification of a lubricant transfer process that enhances the sliding life of a $MoS_2$ coating, *Tribol. Lets., 1* (1995) 59-66.
[26] K.J. Wahl and I.L. Singer, Role of the Third Body in Life Enhancement of $MoS_2$, in D. Dowson, *et al.*, (eds.), *The Third Body Concept: Interpretation of Tribological Phenomena*, Vol. 31, Elsevier, Amsterdam, 1996, pp. 407-413.
[27] G.D. Gamulya, G.V. Dobrovol'skaya, I.L. Lebedeva, and T.P. Yukhno, General Regularities of Wear in Vacuum for Solid Film Lubricants Formulated with Lamellar Materials, *Wear, 93* (1984) 319-332.
[28] T. Spalvins, Frictional and Morphological Properties of Au- $MoS_2$ Films Sputtered from a Compact Target, *Thin Solid Films, 118* (1984) 375-384.
[29] I.L. Singer, S. Fayeulle, and P.D. Ehni, Wear behavior of triode-sputtered $MoS_2$ coatings in dry sliding contact with steel and ceramics, *Wear, 195* (1996) 7-20.
[30] G.B. Hopple, J.E. Keem, and S.H. Loewenthal, Development of fracture resistant, multilayer films for precision ball bearings, *Wear, 162-164* (1993) 919-924.
[31] L.E. Seitzman, I.L. Singer, R.N. Bolster, and C.R. Gossett, Effect of a titanium nitride interlayer on the endurance and composition of a molybdenum disulfide coating prepared by ion-beam-assisted deposition, *Surf. Coat. Technol., 51* (1992) 232-236.
[32] S.N. Bunker and A.J. Armini, Modeling of concentration profiles from very high dose ion implantation, *Nucl. Instrum. Methods Phys. Res. B, 39* (1989) 7-10.
[33] J.F. Ziegler, J.P. Biersack, and U. Littmark, *The Stopping and Range of Ions in Solids*. 1985, New York: Pergamon.
[34] D.N. Dunn, L.E. Seitzman, and I.L. Singer, The origin of an anomalous, low $2\theta$ peak in x-ray diffraction spectra of $MoS_2$ films grown by ion beam assisted deposition, *J. Mater. Res., 12* (1997) 1191-1194.
[35] R.N. Bolster, I.L. Singer, J.C. Wegand, S. Fayeulle, and C.R. Gossett, Preparation by ion-beam-assisted deposition, analysis and tribological behavior of $MoS_2$ films, *Surf. Coat. Technol., 46* (1991) 207-216.
[36] T.J. Weiting and J.L. Verble, Infrared and Raman Studies of Long-Wavelength Optical Phonons in Hexagonal $MoS_2$, *Phys. Rev. B, 3* (1971) 4286-4292.
[37] P.J. Burnett and T.F. Page, An investigation of ion implantation-induced near-surface stresses and their effects in sapphire and glass, *J. Mater. Sci., 20* (1985) 4624-4646.

[38] N.T. McDevitt, M.S. Donley, and J.S. Zabinski, Utilization of Raman spectroscopy in tribochemistry studies, *Wear, 166* (1993) 65-72.

[39] J.S. Zabinski, M.S. Donley, V.J. Dyhouse, and N.T. McDevitt, Chemical and Tribological Characterization of PbO-$MoS_2$ Films Grown by Pulsed Laser Deposition, *Thin Solid Films, 214* (1992) 156-163.

[40] K.J. Wahl, L.E. Seitzman, R.N. Bolster, and I.L. Singer, Low friction, high-endurance, ion-beam-deposited Pb-Mo-S coatings, *Surf. Coat. Technol., 73* (1995) 152-159.

[41] D.N. Dunn, K.J. Wahl, and I.L. Singer, Nanostructural Aspects of Wear Behavior in Ion-Beam Deposited Pb-Mo-S Films, in N.R. Moody, *et al.*, (eds.), *Fundamentals of Nanoindentation and Nanotribology*, Vol. 522, Materials Research Society, Pittsburgh, PA, 1998, pp. 451-456.

[42] K.J. Wahl, D.N. Dunn, and I.L. Singer, Wear behavior of Pb-Mo-S Solid Lubricating Coatings, *Wear, 230* (1999) 175-183.

[43] K. Suzuki, M. Soma, T. Oniski, and K. Tamaru, Reactivity of molybdenum disulfide surfaces studied by XPS, *J. Electron. Spectrosc. Relat. Phenom., 24* (1981) 283-287.

[44] P.D. Fleischauer and R. Bauer, The Influence of Surface Chemistry on $MoS_2$ Transfer Film Formation, *ASLE Trans., 30* (1987) 160-166.

[45] P.J. Burnett and T.F. Page, Changing the surface mechanical properties of silicon and $\alpha$-$Al_2O_3$ by ion implantation, *J. Mater. Sci., 19* (1984) 3524-3545.

[46] C.J. McHargue, The Mechanical Properties of Ion Implanted Ceramics - A Review, *Defect and Diffusion Forum, 57-58* (1988) 359-380.

[47] P.J. Burnett and G.A.D. Briggs, The elastic properties of ion-implanted silicon, *J. Mater. Sci., 21* (1986) 1828-1836.

[48] C.J. McHargue, Ion implantation in metals and ceramics, *Int. Metals Reviews, 31* (1986) 49-76.

**FIGURES**

Figure 1. 360 keV $Ar^{+}$ implantation profiles of $MoS_2$ coated Si at the four doses indicated. Computations assumed atomic densities of 4.8 g/cm$^3$ for $MoS_2$ and 2.3 g/cm$^3$ for Si and pre-irradiation coating thickness of 185 nm. Final thickness (shown) includes sputtering loss.

Figure 2. Schematic diagram of reciprocating sliding 'stripe' tests. Arrow marked "start" indicates test starting location, turnaround points are indicated by open circles, and sliding cycles for the track segments are numbered.

Figure 3. (a) XRD and (b) Raman spectra from IBAD $MoS_2$ coatings, as-deposited and ion irradiated with 180 keV $Ar^{++}$ ions.

Figure 4. Cross-section TEM images from IBAD $MoS_2$ coatings (a) as-deposited, and after irradiation with 180 keV $Ar^{++}$ ions to (b) $1x10^{15}$ ions/ cm$^2$ (LD) and (c) $5x10^{16}$ ions/ cm$^2$ (UHD). Fringes running left to right correspond to $MoS_2$ basal planes (S-Mo-S).

Figure 5. Unidirectional (POD) and reciprocating sliding endurance for as-deposited and ion irradiated IBAD $MoS_2$ coatings.

Figure 6. Friction coefficient evolution for reciprocating sliding in dry air against (a) as-deposited, (b) $1x10^{16}$ ions/ cm$^2$ (HD) and (c) $5x10^{16}$ ions/ cm$^2$ (UHD) $MoS_2$ coatings.

Figure 7. Wear track depths measured by interference microscopy for as-deposited and ion irradiated IBAD $MoS_2$ coatings. Data points with arrows indicate failure.

Figure 8. Optical micrographs of ball transfer films after 90 cycles of reciprocating sliding for (a) as-deposited, (b) $1x10^{16}$ ions/cm$^2$ (HD) and (c) $5x10^{16}$ ions/ cm$^2$ (UHD) $MoS_2$ coatings.

Figure 9. Wear tracks on flats corresponding to ball transfer films shown in Fig. 8 at 90 cycles and at 900 cycles.

Figure 10. Debris deposited at wear track ends at 30, 300 and 3000 sliding cycles for (a) as-deposited, (b) $1x10^{16}$ ions/ cm$^2$ (HD) and (c) $5x10^{16}$ ions/ cm$^2$ (UHD) $MoS_2$ coatings.

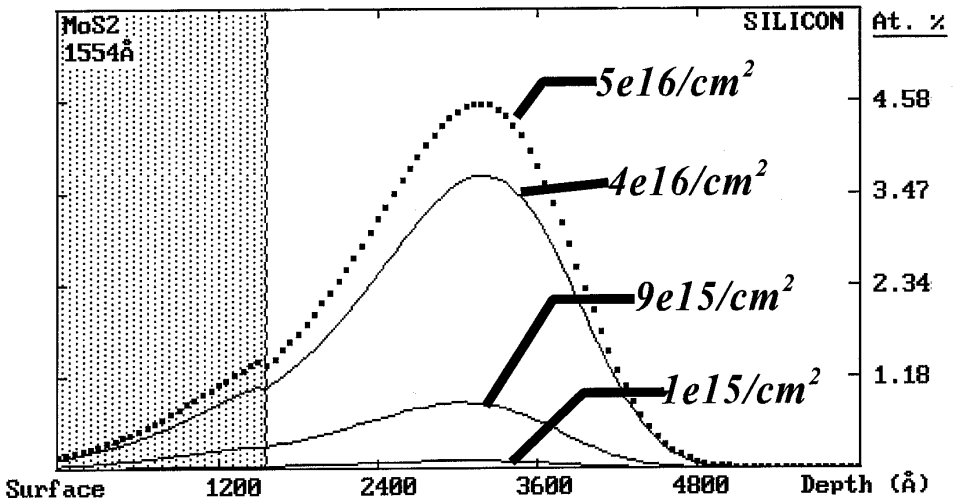


Figure 1. 360 keV $Ar^+$ ion implantation profiles of $MoS_2$ coated Si at the four doses indicated. Computations assumed atomic densities of 4.8 g/cm$^3$ for $MoS_2$ and 2.3 g/cm$^3$ for Si and pre-irradiation coating thickness of 185 nm. Final thickness (shown) includes sputtering loss.

Wahl et al., 1999

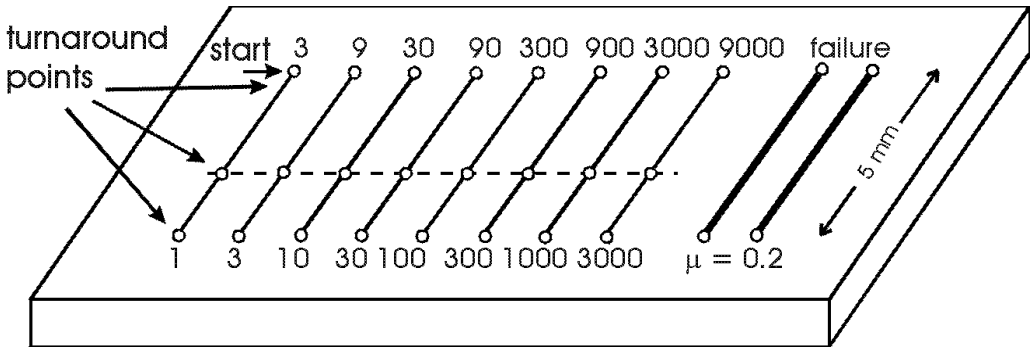


Figure 2. Schematic of reciprocating sliding 'stripe' testing procedure. Arrow marked "start" indicates test starting location, turnaround points are indicated by open circles, and sliding cycles for the track segments are numbered.

Wahl et al., 1999

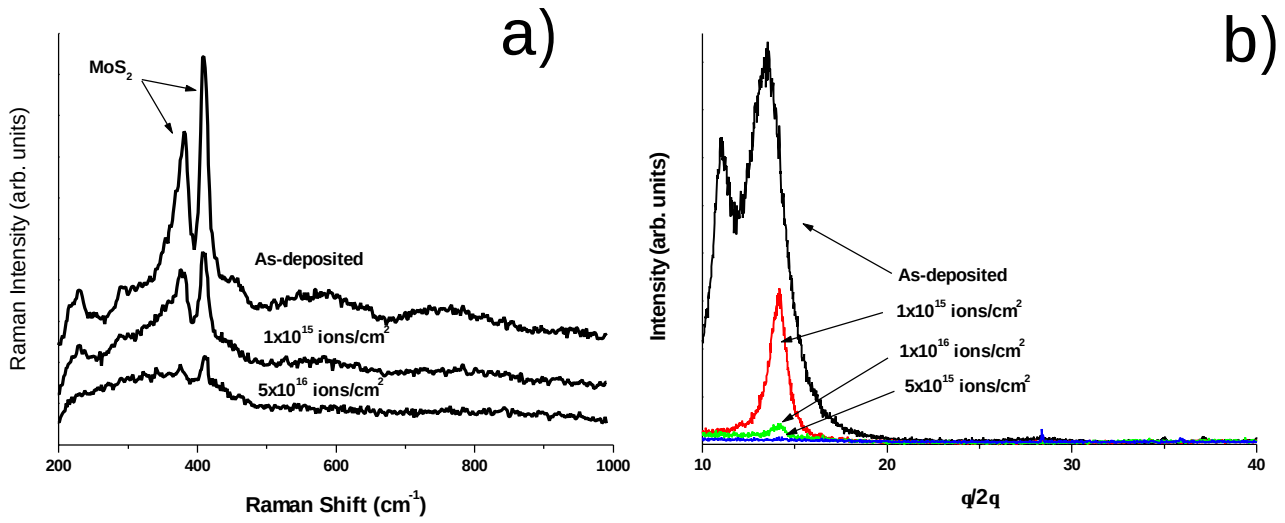


Fig. 3. (a) Raman and (b) XRD spectra of $MoS_2$ coatings, as deposited and ion irradiated with 180 keV $Ar^{++}$ ions.

Wahl et al., 1999

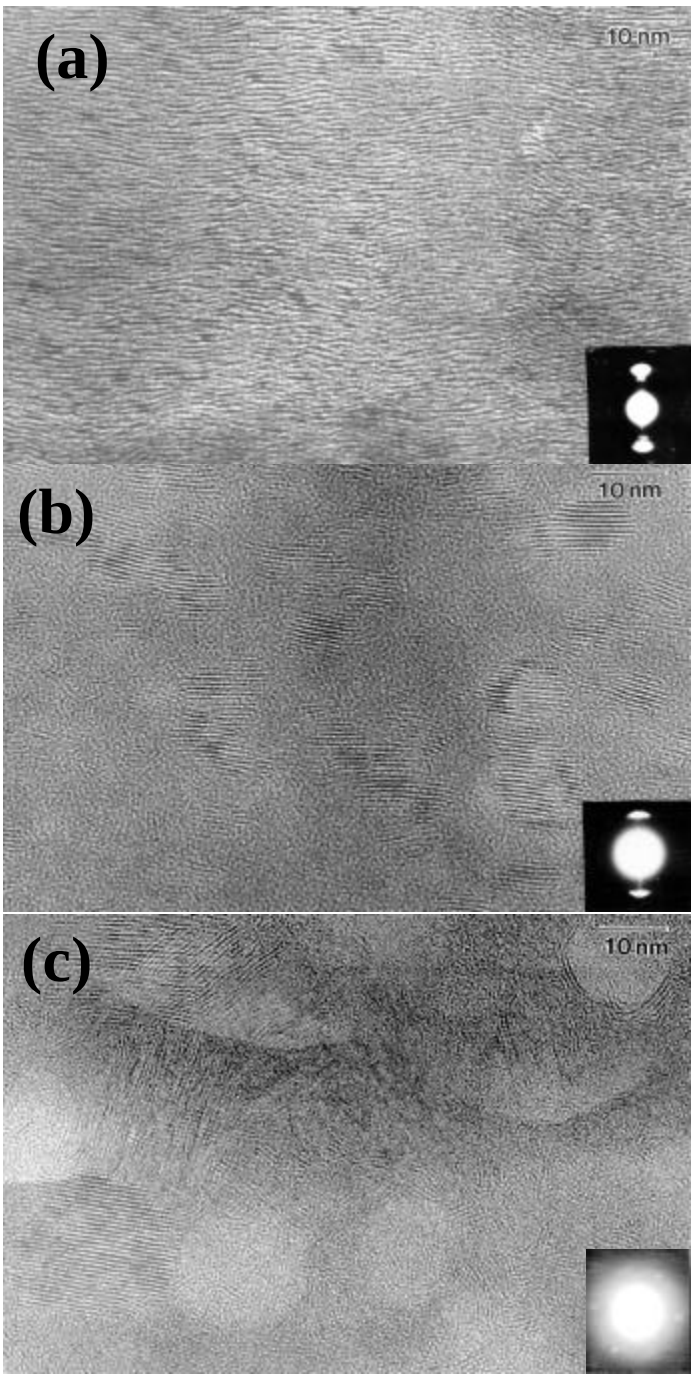


Fig. 4. Cross-section TEM images from IBAD $MoS_2$ coatings (a) as-deposited, and after irradiation with 180 keV $Ar^{++}$ ions to (b) $1x10^{15}$ ions/$cm^2$ (LD) and (c) $5x10^{16}$ ions/$cm^2$ (UHD). Fringes running left to right correspond to $MoS_2$ basal planes (S-Mo-S).

Wahl et al., 1999

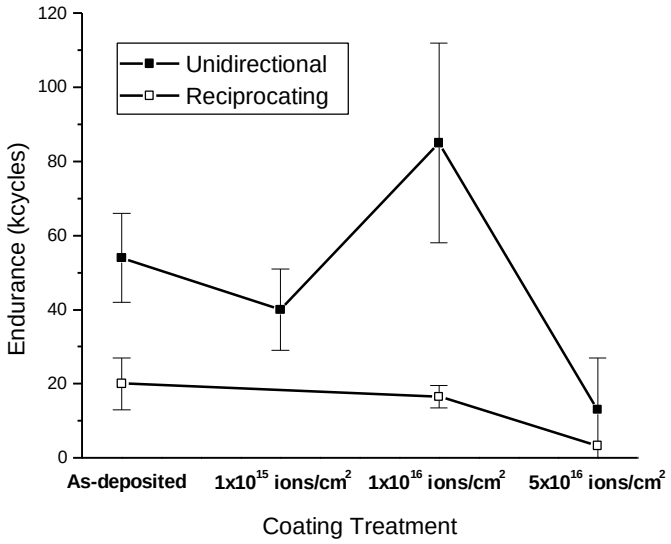


Figure 5. Unidirectional (POD) and reciprocating sliding endurance for as-deposited and ion-irradiated IBAD $MoS_2$ coatings.

Wahl et al., 1999

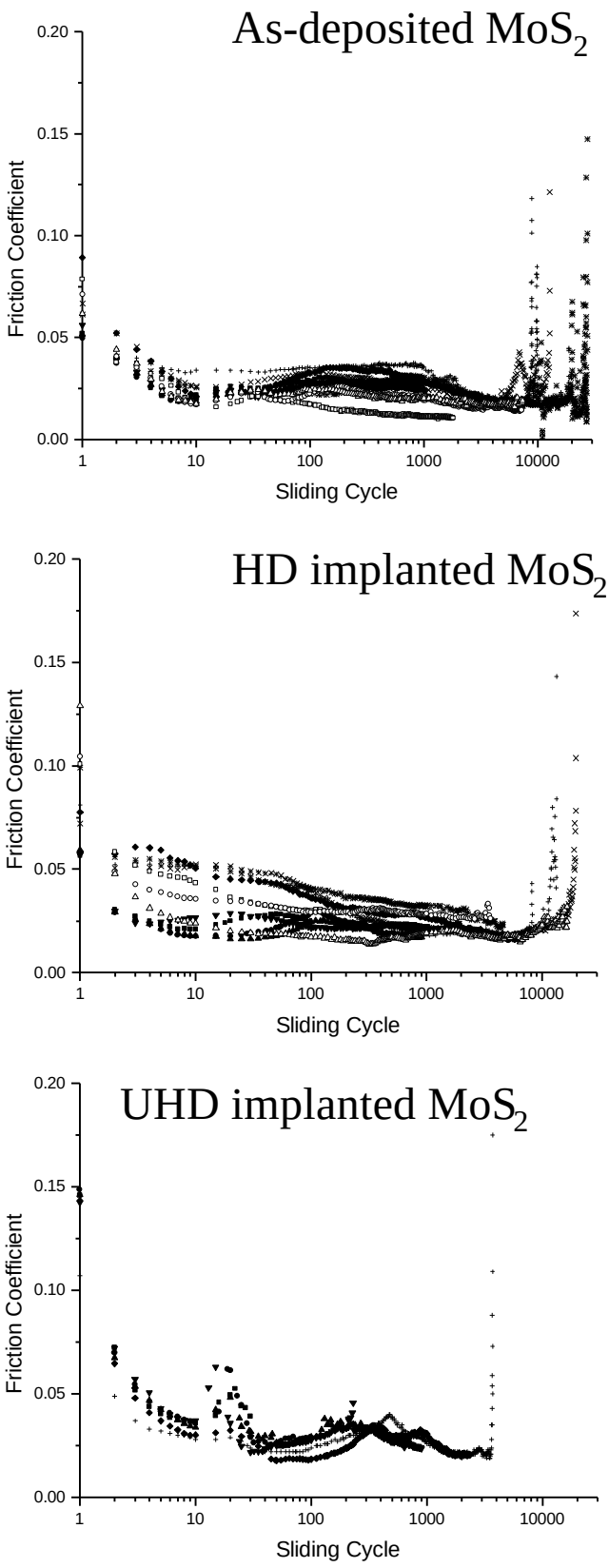


Fig. 6. Friction coefficient evolution for reciprocating sliding in dry air against (a) as-deposited, (b) $1x10^{16}$ ions/cm$^2$ (HD) and (c) $5x10^{16}$ ions/cm$^2$ (UHD) $MoS_2$ coatings.

Wahl et al., 1999

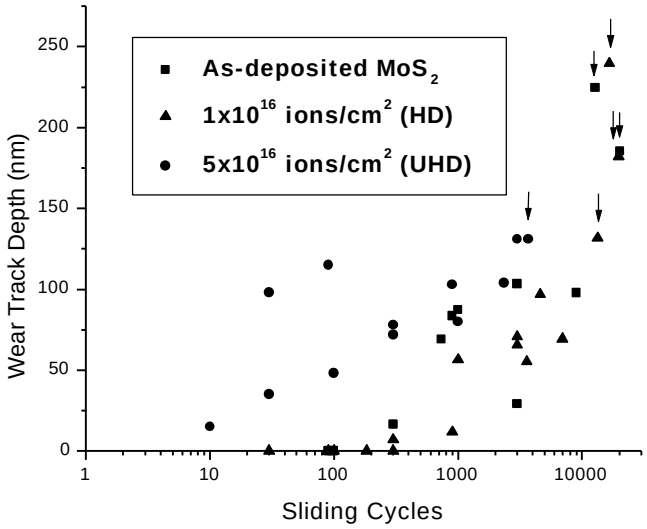


Figure 7. Wear track depths measured by interference microscopy for as-deposited and ion-irradiated IBAD $MoS_2$ coatings. Data points with arrows indicate failure.

Wahl et al., 1999

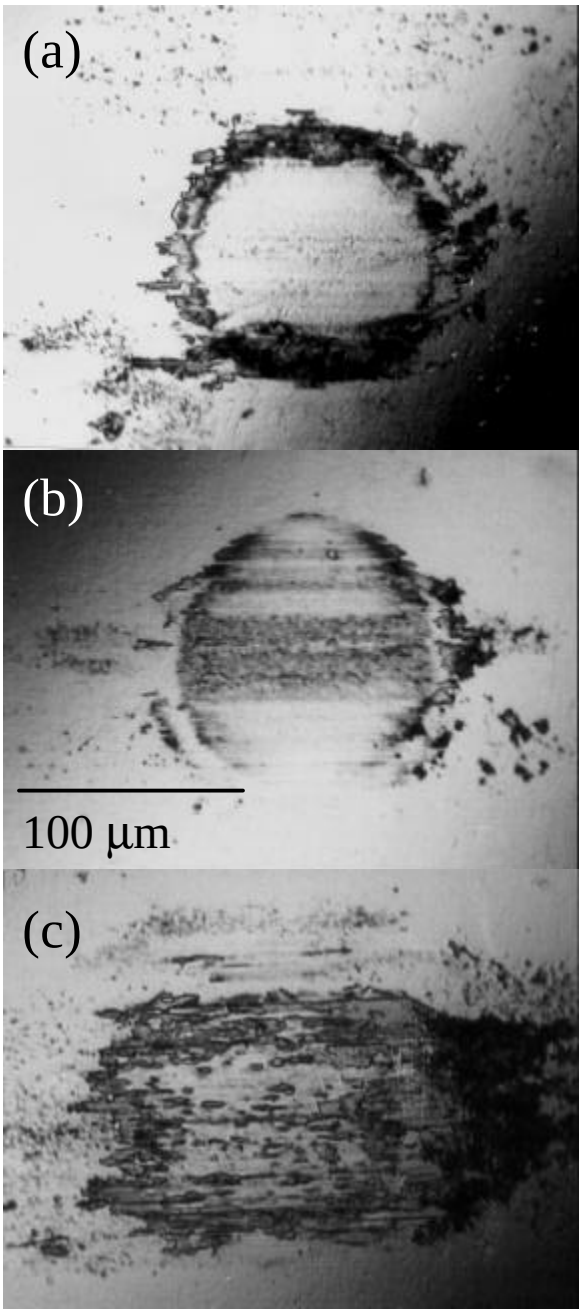


Fig. 8. Optical micrographs of ball transfer films after 90 cycles of reciprocating sliding for (a) as-deposited, (b) $1x10^{16}$ ions/cm$^2$ (HD) and (c) $5x10^{16}$ ions/cm$^2$ (UHD) $MoS_2$ coatings.

Wahl et al., 1999

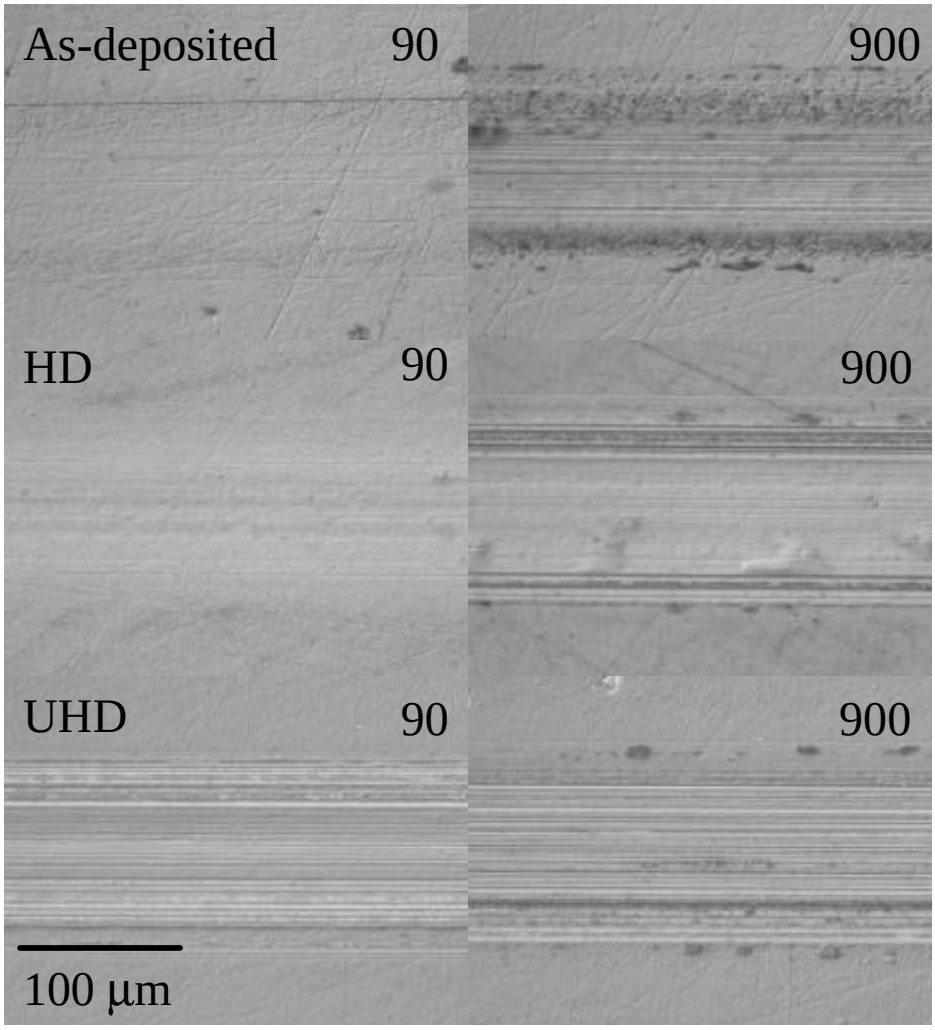


Fig. 9. Wear tracks on flats corresponding to ball transfer films shown in Fig. 8 at 90 cycles and 900 cycles.

Wahl et al., 1999

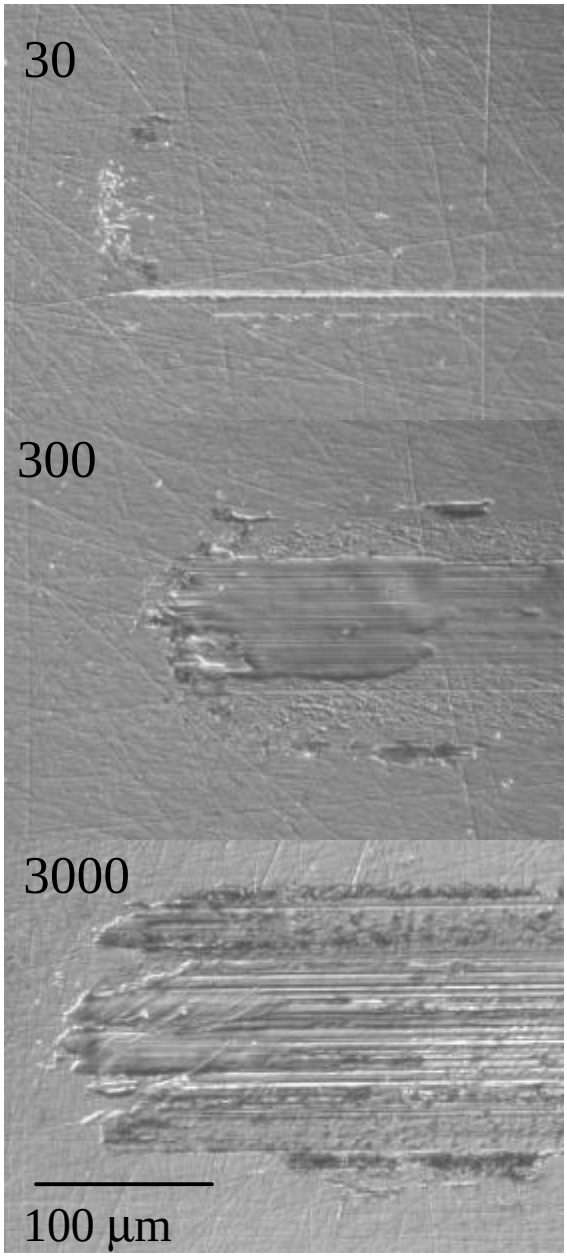


Fig. 10 (a) As-dep $MoS_2$

Wahl et al., 1999

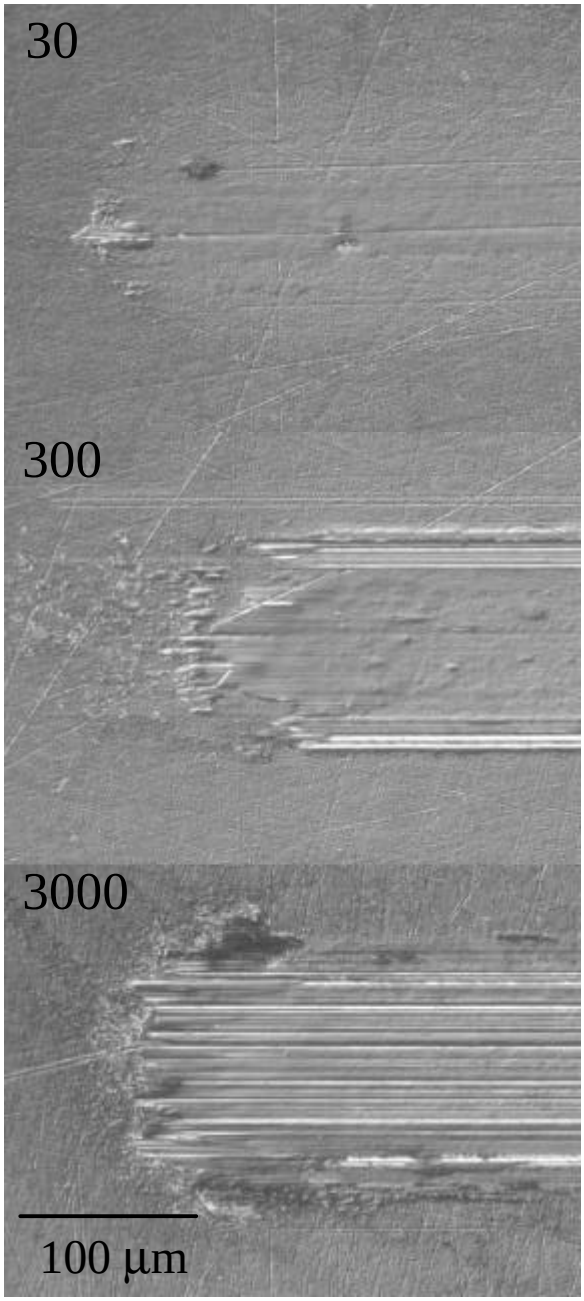


Fig. 10 (b) HD $MoS_2$ Wahl et al., 1999

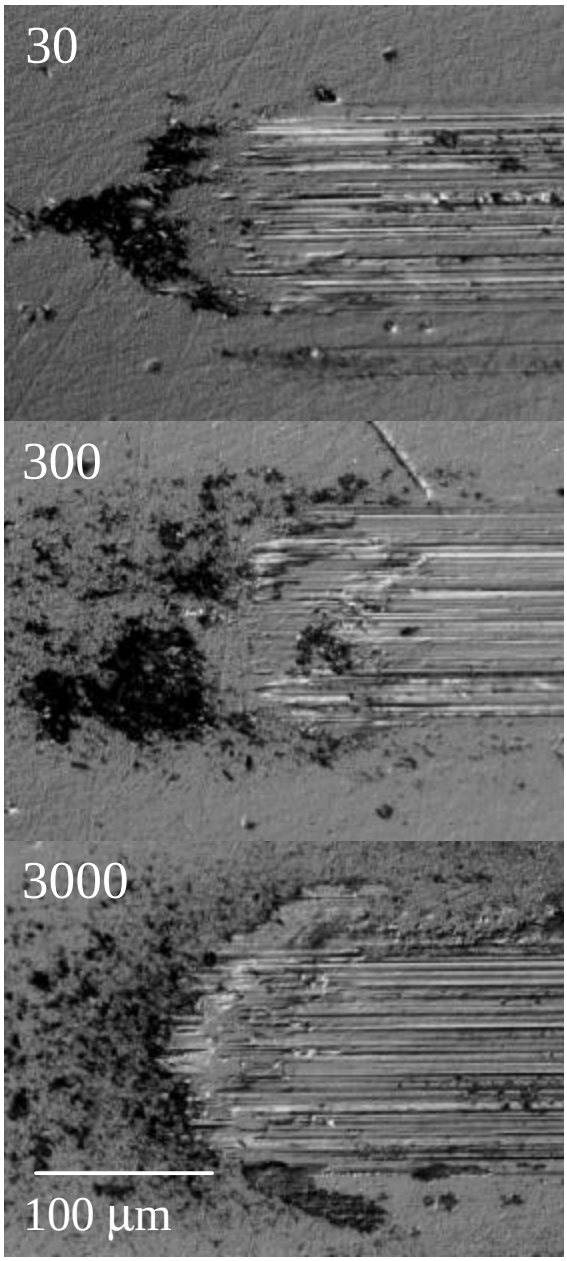


Fig. 10 (c) UHD $MoS_2$

Wahl et al., 1999